ISSN 1027-5495. Functional Materials, 24, No.3 (2017), p. 353-359.
doi:https://doi.org/10.15407/fm24.03.353

Structural aspects of the phase and texture formation processes in thin-layer Ni–W/TiN systems which are perspective for creating high-temperature superconductors of the second generation

M.S.Sunhurov, V.V.Derevyanko, S.A.Leonov, T.V.Sukhareva, V.A.Finkel, Yu.N.Shakhov

National Scientific Center "Kharkiv Physical and Technical Institute",
National Academy of Sciences of Ukraine,
1 Akademicheskaya Str., 61108 Kharkiv, Ukraine

Received February 14, 2017

The investigation objective is searching for the new ways of controlling the structural properties of paramagnetic substrates for creating the high temperature coated superconductors for power applications. Processes of the texture formation in two-component Ni–W/TiN system is studied for paramagnetic Ni — 9.5 at. % W tape with TiN coating, which is deposited by ion-plasma deposition of Ti in nitrogen atmosphere. It is investigated by means of XRD analysis the influence of the deposition time and pressure of nitrogen on the phase and cubic texture formation in the both subsystems of Ni — 9.5 at. % W/TiN. It is found the effect of the crystal planes reorienting in the tape of Ni — 9.5 at. % W under the influence of TiN coating, that leads to a substantial strengthening of the cubic texture of the metallic ribbon. It is also observed the difference in the mechanism of coating formation during the deposition of TiN on the front and the back(shady) side of the substrate. It is also revealed that optimization of the conditions of thin TiN layer deposition makes it possible to obtain quasi single crystalline TiN coatings with a cubic texture. These textured Ni — 9.5 at. % W/TiN substrates admit the epitaxial growth of the high quality HTS films with high current carrying capacity.
Keywords: 2G HTS; texture; Ni — 9.5 at. % W alloy; TiN buffer layer; paramagnetic substrate.

Осуществлен поиск новых путей управления структурными свойствами парамагнитных подложек для создания высокотемпературных пленочных сверхпроводников. Методами рентгеноструктурного анализа изучены процессы текстурообразования в тонкопленочной двухкомпонентной системе на основе металлической подложки из парамагнитного сплава Ni — 9.5 at. % W с буферным покрытием TiN, которое нанесено методом ионно-плазменного осаждения Ti в атмосфере азота. Исследовалось влияние времени осаждения TiN и величины давления паров азота на процессы фазообразования и формирования кубической текстуры в обеих компонентах тонкослойной системы "Ni — 9.5 at. % W/TiN". Обнаружены отличия в механизме формирования покрытия при осаждения TiN на лицевую и теневую стороны подложки. Обнаружен эффект переориентации кристаллических плоскостей в ленте сплава Ni — 9.5 at. % W под воздействием покрытия, ведущий к существенному усилению кубической текстуры металлической подложки. Показано, что при оптимизации условий нанесения тонкослойного покрытия в системе "Ni — 9.5 at. % W/TiN" имеет место формирование квазимонокристаллических слоев TiN с кубической текстурой.

Структурні аспекти процесів фазоутворення та формування текстури у тонкошарових системах Ni–W/TiN, перспективних для створення високотемпературних надпровідників другого покоління. *М.С.Сунгуров, В.В.Дерев'янко, С.О.Леонов, Т.В.Сухарєва, В.О.Фінкель, Ю.М.Шахов.*

Здійснено пошук нових шляхів керування структурними властивостями парамагнітних підкладок для створення високотемпературних плівкових надпровідників. Методами рентгеноструктурного аналізу вивчено процеси формування текстури у тонкошаровій двокомпонентній системі на основі металевої стрічки з парамагнітного сплаву Ni — 9.5 at. % W із буферним покриттям TiN, яке наносилося методом іонно-плазмового осадження Ti в атмосфері азоту. Досліджено вплив часу осадження TiN і величини тиску парів азоту на процеси фазоутворення і формування кубічної текстури в обох компонентах тонкошарової системи "Ni — 9.5 at. % W/TiN". Виявлено відмінності у механізмі формування покриття при осадження ÒiN на лицьову і тіньову сторони підкладки. Виявлено ефект переорієнтації кристалічних площин у стрічці сплаву Ni — 9.5 at. % W під впливом покриття, що веде до істотного посилення кубічної текстури металевої підкладки. Показано, що при оптимізації умов нанесення тонкошарового покриття у системі "Ni — 9.5 at. % W/TiN" має місце формування квазімонокристалічних шарів TiN з кубічною текстурою.

1. Introduction

Research and development [1–3] in the field of creating the high-temperature superconductors of the second generation (2G HTS) based on HTS YBCO [4] textured films is of particular interest, because it opens up the new perspectives for creating the superconductors, which could work at the temperature of liquid nitrogen boiling point (77.4 K).

Architecture of 2G HTS [5] with expected critical current density $j_c \sim 10^5 - 10^6$ A/cm^2 consists of:

base (a thin tape of Ni–W alloys with different composition or other alloys with FCC crystal structure);

buffer layer/layers (oxides, nitrides, in particular TiN [6], due to having FCC structure and acceptable mechanical properties);

single crystalline superconducting film $YBa_2Cu_3O_{7-\delta}$ (YBCO) with $T_c \sim 92$ K (the rhombic lattice, space group $P4/mmm$).

The metallic base of substrate [7, 8] plays an extremely important role in creation of effective 2G HTS: Ni–W ribbon should possess both the strong {100}<001> texture (to provide the formation of biaxial cube texture in the film of superconductor because of the epitaxial growth of superconductive layer on the substrate) and be in paramagnetic state [9] (to decrease the level of ferromagnetic loses during passing the alternating current over the superconducting film).

The paramagnetism of Ni–W is provided by increasing the concentration of W in the alloy up to 9.5 at. % W. The main obstacle for production of paramagnetic Ni–W tapes with cubic texture is the low value of stacking faults energy E_{sf}, which decreases with increasing the content of tungsten in the alloy and restrains formation of the sharp cubic texture [10].

Previously in our investigations the effects of texture formation in both components of the system "paramagnetic tape Ni — 9.5 at. % W/TiN coating" have been already demonstrated [11–13]. The main aim of this work is to find the new ways of controlling the structural properties of substrates for creation of high-temperature superconductors with the high current-carrying capacity (2G HTS). To achieve the goal it is necessary to solve the following tasks:

1. Investigation of the phase constitution of Ni–W alloys in the wide range of W concentration and production of tapes based on Ni–W alloys in accordance with the received data. Conducting this research makes it possible to establish the range of concentrations of tungsten in the Ni–W alloys suitable to produce paramagnetic substrates with desired properties.

2. Optimization of the deposition parameters of titanium nitride coating with TiN plasma deposition method onto Ni–W tapes to ensure the possibility of obtaining the cubic texture in the both components of the system "paramagnetic Ni–W substrate/thin TiN coating".

3. Study of influence of TiN deposition parameters (pressure $p(N_2)$ and deposition time τ_{TiN}) will provide the information on possible mechanisms of phase and texture formation in the both subsystems of "paramagnetic Ni–W tape/TiN coating".

2. Experimental

Preparation and validation of substrates were carried out according to the scheme which includes the following steps: 1) synthesis of Ni–W alloys in the wide range of W concentrations; 2) thin-layer tape production; 3) deposition of TiN coating; 4) XRD analysis.

2.1. Preparation of Ni–W alloys with different compositions (0 to 25 at. % W)

Initial materials for obtaining the Ni–W alloys were Ni and W powders with 99.98–99.99 % purity (by metallic impurities). The following methods were used for purification from gaseous impurities: 1) heat treatment in vacuum at temperatures ~ 850°C for purification of Ni powder [14]; 2) for refinement of W powder it was applied the high-temperature treatment (1000–1200°C) in recovering Ar + 4 % H_2 gaseous mixture flow [15]. After the thermal treatment in such environment the effects of oxidation at microscopic examination were not observed, evidently due to passivation of the surface grains of tungsten. After the refinement the Ni and W powders were thoroughly mixed in necessary proportions (0, 2.5, 5, 7.5, 9.5, 15, 20, and 25 at. % W) and pressed into bars (2×10×50 mm^3). The Ni–W alloys were synthesized by means of powder metallurgy in deep vacuum (p ~ 10^{-6} Torr) at T = 1200°C during t = 4 hours.

2.2. Production of thin-layer Ni–W ribbon

Obtained ingots were rolled up to 50–100 μm at the room temperatures by "extreme rolling procedure" [12], i.e., realizing the large number of rolling acts with the low deformation without intermediate annealing. The total degree of cold-rolling deformation was about 95 %. The resulting operation during the tape production was the high-temperature annealing at T = 1150°C during t = 2 hours in the reducing atmosphere of Ar + 4 % H_2.

2.3. Deposition of TiN coating on the surface of Ni–W tapes

Thin layers of titanium nitride (TiN) on the surface of Ni–W tapes were obtained by method of ion-plasma deposition [16–19]. The experimental parameters were as follow: negative substrate potential U = – 300 V; arc current I = 80 A; nitrogen pressure in a chamber $p(N_2)$ = 1.2 – 6.2·10^{-2} Torr; time of deposition τ_{TiN} = 60–900 s. As a rule the coating is applied to the front side of the substrate, i.e. facing towards the cathode. At the same time there is tecnically possible the deposition of TiN onto the back or shady side of the substrate out of the direct vision of plasma source. To enhance the control options of structure and properties of the two-component Ni–W/TiN substrates, experiments on TiN coating deposition on the shady side as well as on the front side of the Ni–W tape were carried out. But it should be mentioned that proposed type of deposition on the back side is of primary interest in the present work.

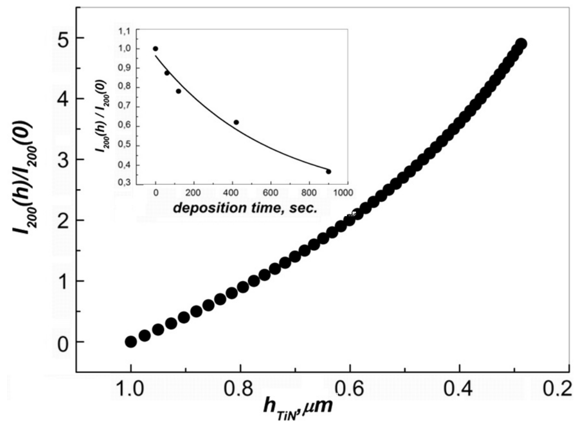

Fig. 1. Determination of coating thickness of TiN: nomogram for (200) plane.

2.4. Features of X-ray diffraction studies in relation to thin-layer two-component systems of Ni–W/TiN

XRD analysis (diffractometer DRON UM-1, Cu Kα radiation) was used to solve the following tasks: determination of the phase composition, determination of the lattice parameters of Ni–W and TiN, determination of TiN layer thickness, studying the texture of the both components of the system Ni–W/TiN.

2.4.1. Determining the thickness of the coating layer

The method of determination the TiN-layer thickness is based on the effects of X-ray absorption [20–23]. Intensity of beam reflected from crystal plane (hkl) of a sample with the coating thickness h is as follows:

$$I_{hkl}(h) = I_{hkl}(0) \cdot \exp\left(-2h \cdot \mu_{TiN}/\cos(\theta)\right), \quad (1)$$

$I_{hkl}(h)$ — intensity of the beam reflected from the substrate with coating; $I_{hkl}(0)$ — intensity of the beam reflected from the substrate without coating; h — coating layer thickness; μ_{TiN} — linear absorption co-

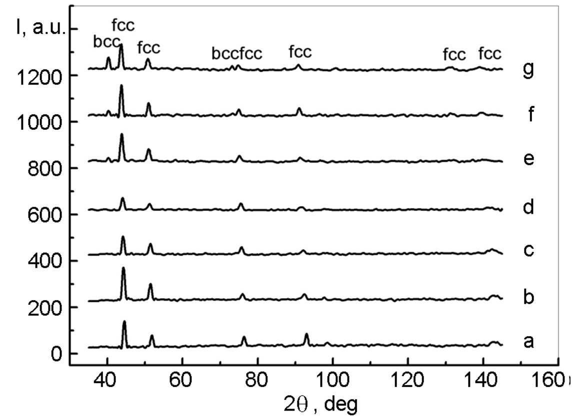

Fig. 2. XRD patterns from the bars of Ni–W alloys with different compositions: a — 0 at. % W; b — 5 at. % W; c — 9.5 at. % W; d — 15 at. % W; e — 20 at. % W; f — 25 at. % W.

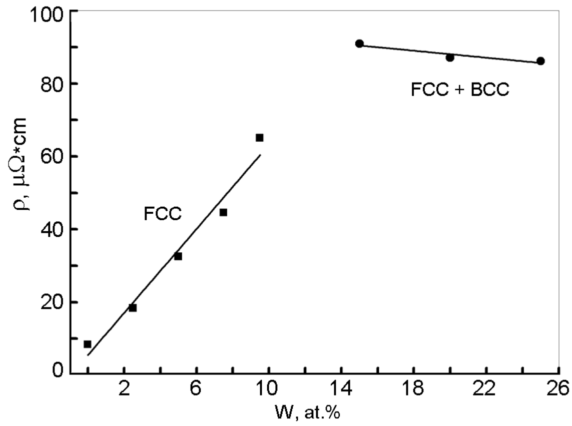

Fig. 3. Resistivity of Ni–W alloys with different content of tungsten. FCC — face centered cubic lattice, BCC — body centered cubic.

efficient of the coating material; θ — the Bragg angle.

Equation (1) and mathematical modeling of the relative intensity of some X-ray interferences, makes it possible to determine the coating thickness h_{TiN} within ~ 10 %. Fig. 1 illustrates the relationship between intensity of some diffraction lines from Ni–W substrate and thickness of TiN layer deposited on it. Although the absorption coefficient for the cubic lattice is isotropic, as stated previously in the Ni — 9.5 at. % W tape the processes of crystal grains reorientation may occur, that should lead to change in the diffraction intensity. All thickness measurements are advisable to carry out on test samples. In the present study for TiN thickness measuring the samples of Ni — 5 at. % W tapes are used, because of presence stable and sharp cubic texture, which doesn't show any appreciable deviations during deposition process.

2.4.2. Texture analysis of obtained samples

In order to determine fine variations of rather strong textures in the Ni–W/TiN system, classical methods were supplemented by an algorithm of planar texture characterization based on construction and analysis of diagrams of the angular distribution of intensities from crystallographic planes [13]. In the present work it was most important to study the cubic planes (200) of FCC lattices of the metallic ribbon and coating in various directions. Samples were rotated by angle φ about the normal direction at 15° step. The validity of the hypothesis of realization of the perfect cubic texture was verified using χ^2 method. The χ^2 value was calculated for $n = 23$ degrees of freedom. For example the χ^2 value for the test sample Ni — 5 at. % W with strong cubic texture is equal to 0.022.

3. Results

This section presents experimental results obtained in accordance with the research program.

3.1. Influence of chemical composition on the crystal structure and electro-physical properties of Ni–W alloys

For attestation of the samples it was necessary to consider concentration dependences of structural properties and resistivity. Fig. 2 illustrates a set of diffraction patterns of the Ni–W alloys with different composition. Within the range of tungsten concentrations from 0 to 9.5 at. % W there are observed only diffraction lines of single-phase FCC solid solution of W in Ni. At the concentration of about 15 at. % W and higher on XRD patterns the lines belonging to BCC phase of solid solution of Ni in W appear. Another concentration dependence is shown in Fig. 3. As it can be seen the resistivity curve shows practically linear growth with increasing the concentration of tungsten in the alloy up to 15 — at. % W. In the region, where the Ni–W alloy is in two-phase state, the resistivity slightly decreases. Further research was performed on the specimens of Ni — 9.5 at.% W alloy, that is in the paramagnetic state over the entire temperature range and is in the boundary of the single phase region.

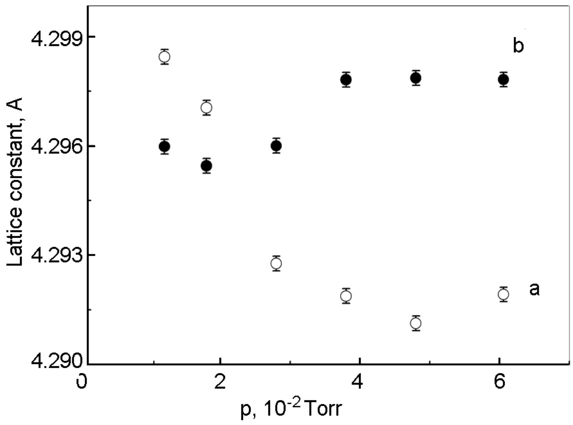

Fig. 4. Lattice parameters change of TiN layer deposited on Ni — 9.5 at. % W tape at different pressures of nitrogen $p(N_2)$: a) front side; b) shady side.

3.2. Influence of conditions of TiN deposition on the crystal structure of two-component system Ni — 9.5 at % W/TiN

In the present study the TiN coating was deposited on the front and the shady side of Ni — 9.5 at. % W substrate. In accordance with the research program two series of experiments on deposition were carried out: in the range of nitrogen pressures at constant process time τ_{TiN} = const and in the range of times at constant pressure $p(N_2)$ = const.

3.2.1. TiN deposition at constant time τ_{TiN} ~600 sec in a wide range of pressures of nitrogen $p(N_2) = 1.2–6.2 \cdot 10^{-2}$ Torr

Based on the received data in Fig. 4 there are shown dependences of TiN lattice constant a_{TiN} on the pressure of nitrogen $p(N_2)$ at different geometries of the experiment on deposition. The behavior of a_{TiN} variations essentially differs at $p(N_2) > 1.8 \cdot 10^{-2}$ Torr. The crystal lattice parameter a_{TiN} of the coating layer, which was deposited on the front side of the Ni — 9.5 at. % W tape decreases with increasing pressure practically over the whole range. The value a_{TiN} of the TiN layer on the shady side of the substrate tends to increase at $p(N_2) > 1.8 \cdot 10^{-2}$ Torr. Possible nature of this observation will be discussed below (see Discussion).

Another important observation is the redistribution of the intensity of Ni–W lines in the diffraction pattern. Fig. 5 illustrates relationship between the values of cubic plane intensity (as a "texture parameter" was chosen ratio I_{200}/I_{220}) and pressure $p(N_2)$ at deposition on the face and shady side of the Ni — 9.5 at. % W substrate.

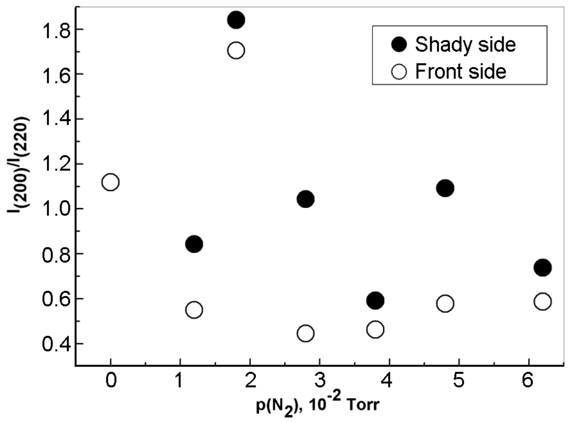

Fig. 5. Values of ratio I_{200}/I_{220} for the front and shady sides of the Ni — 9.5 at. % W substrate at different pressures of nitrogen.

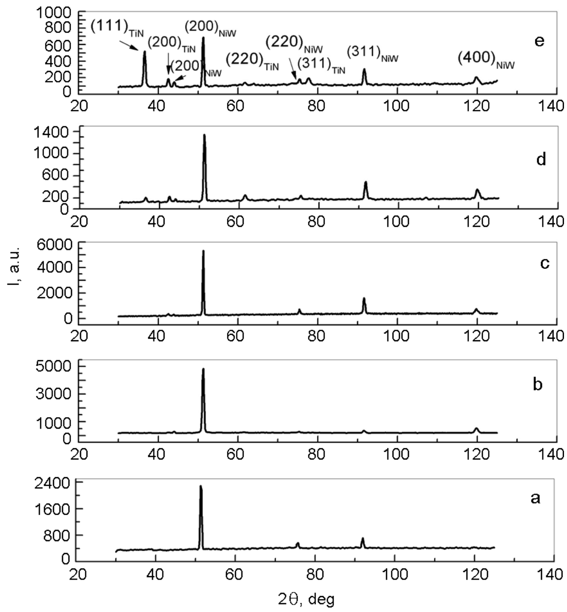

Fig. 6. XRD patterns of Ni — 9.5 at. % W alloy tapes with TiN coating (shady side of the substrate) at $p(N_2) = 1.8 \cdot 10^{-2}$ Torr in the range of deposition times: a) τ_{TiN} = 0 sec; b) τ_{TiN} = 60 sec; c) τ_{TiN} = 120 sec; d) τ_{TiN} = 420 sec; e) τ_{TiN} = 900 sec.

Dependences have nonmonotonic character. At nitrogen pressure $p(N_2) = 1.8 \cdot 10^{-2}$ Torr the both curves have the maximum. Obviously this pressure can be considered as the optimal for the most suitable development of the cubic texture, it was used as a fixed parameter in the second series of experiments.

3.2.2. TiN deposition at pressure of nitrogen $p(N_2) = 1.8 \cdot 10^{-2}$ Torr in the range of times τ_{TiN} = 60–900 sec

It was important to study the influence of process time on the crystal structure of

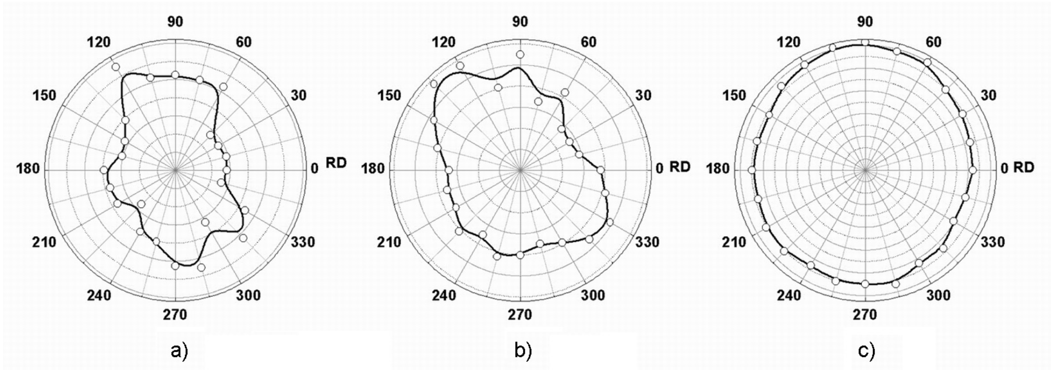

Fig. 7. Circular diagrams of (200) planes related to formation of sharp cubic texture at $p = 1.8\cdot10^{-2}$ Torr and h_{TiN} ~ 0.8 μm for: a) Ni — 9.5 at. % W ($\chi 2$ = 0.082); b) Ni — 9.5 at. % W under coating ($\chi 2$ = 0.045); c) TiN layer ($\chi 2$ = 0.004).

both components of the system "The paramagnetic tape Ni – 9.5 at. % W/TiN layer". Evolution of the diffraction pattern for "shady geometry" depending on the TiN deposition time at constant pressure of nitrogen is plotted in Fig. 6. There are two systems of diffraction lines, belonging to the FCC lattice of Ni — 9.5 at. % W alloy and NaCl-type TiN lattice. As the deposition time τ_{TiN} increases in other words as the TiN thickness h_{TiN} growths the texture of Ni — 9.5 at. % W ribbon exhibits variations. As seen on the graph there takes place intensification of $(h00)_{Ni-W}$ type diffraction lines up to τ_{TiN} = 120 sec (h_{TiN} ~ 0.8 μm). The processes of the cubic texture formation are also observed in the coating layers of TiN. This is proved by the presence of only $(200)_{TiN}$ reflex, which belongs to the cubic plane of the TiN lattice. In Fig. 7 it is shown a set of circular diagrams also indicating the process of texture formation in the system "Ni — 9.5 at. % W/TiN" in the case of shady geometry. Further increase of τ_{TiN} leads to deterioration of texture quality in the both subsystems, accompanied by decreasing of $I_{(200)}$ intensity from the Ni–W phase as well as appearance of the non cubic lines of titanium nitride.

4. Discussion

The following observed effects can serve as the subject of discussion:

Formation of rather strong cube texture in the surface layer of Ni — 9.5 at. % W tape under the effect of TiN coating.

Formation of quasi mono crystalline structure of TiN buffer layer in the system Ni — 9.5 at. % W/TiN.

Existence of qualitative changes of the crystal lattice parameter dependences of titanium nitride on nitrogen pressure at different "geometry" of the experiment on TiN deposition.

Significant differences in the value of the crystal lattice parameters of Ni — 9.5 at. % W and TiN may cause mechanical stresses at the interface between the two phases. It is natural to assume that in the field of elastic stresses there is an increase of stacking faults energy E_{sf}, which provides potential possibility of the cubic texture formation in the metallic component of Ni — 9.5 at. % W/TiN system. Formation of the quasi single crystalline structure (h00) in the layers of titanium nitride can also be linked to emergence of the shot-range strains in the two-component system.

In the standard geometry of the experiment (deposition on the substrate front side) due to sufficiently large thickness of TiN layer, the choice of parameters, for which the favorable conditions for increasing of E_{sf} are realized, is limited by technical difficulties (since the both texture effects associated with the tape of Ni — 9.5 at. % W and TiN layer are realized in a narrow range of values of the TiN deposition times). While the application of "shadow" geometry makes it possible to select the conditions ensuring the strong cube texture in both components of the thin-layer system Ni — 9.5 at. % W/TiN more accurately.

It is evident that the features of texture formation within Ni–W/TiN system are associated not only with the change of the coating thickness, but also with the compositional change of titanium nitride at the different deposition geometry. Variations of the crystal lattice parameters of TiN depending on the pressure of nitrogen vapor and geometry of the experiment indicate a change in the kinetics of the phase formation of titanium nitride. Within the range of pressures $p(N_2)$ ~ $1.8 - 2.8 \cdot 10^{-2}$ Torr the composition of TiN phase is changing. Dependence on the front side of the substrate reflects the increase of the Ti content in the coating composition, whereas on the shady side of the substrate the decrease of Ti content is observed.

5. Conclusions

Fundamental results obtained in this work are related to establishing the regularities of changing of crystal structure within two-component system "Ni — 9.5 at. % W/TiN": formation of cubic texture in the both subsystems; maximum degree of the cube texture in Ni — 9.5 at. % W and TiN is realized at different coating thicknesses; the kinetics of the formation and composition of the titanium nitride phase depends on the geometry of the TiN coating experiment. Results of the study indicate that the tapes of paramagnetic Ni — 9.5 at. % W with TiN coating can be considered as promising substrates for creating the effective 2G HTS superconductors.

References

1. A.Goyal, D.Norton, D.Kroeger et al., *J. Mater. Res.*, **12**, 2924 (1997).
2. A.Goyal, D.Lee, F.List et al., *Physica C*, **357**, 903 (2001).
3. A.Vanozzi, A.Rufoloni, G.Celentano et al., *Supercond. Sci. Technol.*, **19**, 1240 (2006).
4. M.W.Rupich, *Supercond. Sci. Technol.*, **23**, 014015 (2010).
5. D.Larbalestier, A.Gurevich, D.Feldmann, A.Polyanski, *Nature*, **414**, 368 (2001).
6. R.Huhne, K.Guth, R.Gartner et al., *Supercond. Sci. Technol.*, **23**, 014010 (2010).
7. A.O.Ijodola, J.R.Thomson, A.Goyal, *Physica C*, **403**, 163 (2004).
8. Y.A.Ganenko, H.Rauch, P.Kruger, *Appl. Phys. Lett.*, **98**, 152303 (2011).
9. V.S.Sarma, J.Eickemeyer, L.Schultz, B.Holzapfel, *Scr. Mater.*, **50**, 953 (2004).
10. F.A.Mohamed, T.G.Langdonm, *Met. Trans. V.*, **5A**, 927 (1978).
11. V.A.Finkel, A.M.Bovda, S.A.Leonov et al., *Functional Materials*, **19**, 109 (2012).
12. V.A.Finkel, V.V.Derevyanko, M.S.Sunhurov et al., *Functional Materials*, **20**, 103 (2013).
13. M.S.Sungurov, V.V.Derevyanko, S.A.Leonov et al., *Techn. Phys. Lett.*, **40**, 817 (2014).
14. F.P.Larkins, P.J.Fensham, *Nature*, **215**, 1268 (1967).
15. H.L.Suo, Y.Zhao, M.Liu, *Supercond. Sci. Technol.*, **21**, 075003 (2008).
16. I.I.Axenov, V.G.Padalka, A.N.Belokhvostikov et al., *Plasma Physics and Controlled Fusion*, **28**, 761 (1986).
17. I.I.Axenov, V.M.Khoroshikh, *IEEE Trans. Plasma Sci.*, **27**, 1026 (1999).
18. I.I.Axenov, A.A.Andreev, A.A.Romanov et al., *Ukr. Phys. Journal*, **24**, 515 (1979).
19. V.M.Khoroshikh, S.A.Leonov, V.A.Belous, *Probl. Atomic Sci.&Techn. Ser. Vacuum, Pure Mater., Supercond.*, No. 1, 72 (2008).
20. Y.S.Liu, Y.Zhao, *Textures and Microstructures*, **30**, 71 (1997).
21. S.Tomov, S.Vassilev, *Solid State Phenomena*, **130**, 43 (2007).
22. H.Friedman, L.S.Birks, *Rev. Sci. Instr.*, **17**, 99 (1946).
24. L.S.Palatnik, *Proc. Kharkiv State University*, **7**, 245 (1950).